

High-pressure studies of NaH to 54 GPa

Steven J. Duclos, Yogesh K. Vohra, and Arthur L. Ruoff

Department of Materials Science and Engineering, Cornell University, Ithaca, New York 14853

S. Filipek and B. Baranowski

Institute of Physical Chemistry, Polish Academy of Sciences, 01-224 Warszawa, Poland

(Received 1 June 1987)

High-pressure x-ray diffraction data on NaH to 54 GPa at room temperature show a $B1(\text{NaCl})$ -to- $B2(\text{CsCl})$ phase transition at $P_T = 29.3 \pm 0.9$ GPa and volume fraction $V/V_0 = 0.61 \pm 0.01$. In the $B1$ phase the isothermal bulk modulus B_0 is 19.4 ± 2.0 GPa, with a pressure derivative B'_0 of 4.4 ± 0.5 . These results, together with earlier measurements on KH, RbH, and CsH, indicate that the alkali-metal hydrides show the same strong dependence of P_T on cation as do the alkali-metal halides. The systematically lower bulk moduli of the alkali-metal hydrides as compared to the alkali-metal halides can be attributed to incomplete charge transfer in this series of partly ionic compounds.

The alkali-metal hydrides (CsH, RbH, KH, NaH, and LiH) represent a series of partly ionic materials whose high-pressure behavior is expected to parallel that of the alkali-metal halides. Specifically, the $B1$ -to- $B2$ phase-transition pressures, which for the non-Li alkali-metal halides range from 0.4 to 30 GPa, are expected to be within the present range of diamond-anvil-cell technology. Hochheimer *et al.*¹ has reported the transition pressures for CsH, RbH, and KH, as well as the equation of state of NaH to 28 GPa. The purpose of the present study is to determine the $B1$ -to- $B2$ transition pressure in NaH. This completes the alkali-metal hydride series (with the exception of LiH, which will probably transform at pressures above current capability, if at all²), and enables us to compare transition pressures, bulk moduli, and effective charges of the alkali-metal hydrides to those of the alkali-metal halides. Such comparisons will lead to an improved understanding of bonding in ionic and partly ionic materials at equilibrium conditions and at high pressures. As an example, Majewski and Vogal³ recently explained the observed $B1$ -to- $B2$ transition pressures using a universal tight-binding model for sp -bonded nonmetals. Further, this study of the weak x-ray scatterer NaH provides experimental verification that structure determinations can be made for materials of low atomic number with the small sample sizes required for ultrahigh-pressure experiments.

The NaH sample was prepared by direct reaction between high-purity gaseous hydrogen and metallic sodium. The metal free hydride was obtained after some hours using a hydrogen pressure of 50 MPa at about 700°C. The reaction product was taken out at ambient conditions in an inert atmosphere of gaseous argon. Two high-pressure experiments were performed on NaH in a gasketed diamond-anvil cell. An initial experiment to 54 GPa used 300- μm flat diamonds, a stainless-steel gasket, and a 50- μm -diam sample hole. This was performed on the hard-bend magnet polychromatic beam line at the Cornell High Energy Synchrotron Source (CHESS), and will be referred to as the "hard-bend run." A second experiment to confirm the transition pressures

and structures used 640- μm flat diamonds, a spring-steel gasket, and a 90- μm -diam sample hole. This was performed on the wiggler polychromatic beam line at CHESS and will be referred to as the "wiggler run." In both experiments a single centered ruby chip was used to determine the pressure from the calibration of Mao *et al.*⁴ Throughout each experiment the R_1 and R_2 ruby-fluorescence lines remained resolved. In both cases 50- μm x-ray collimation was used, and the samples were loaded into the diamond-anvil cell in an inert argon atmosphere to minimize the formation of NaOH. Details of the CHESS energy-dispersive x-ray diffraction (EDXD) setup are given by Brister, Vohra, and Ruoff.⁵

Figure 1 shows two EDXD spectra of NaH taken on the wiggler run, one at 30.1 GPa with NaH predom-

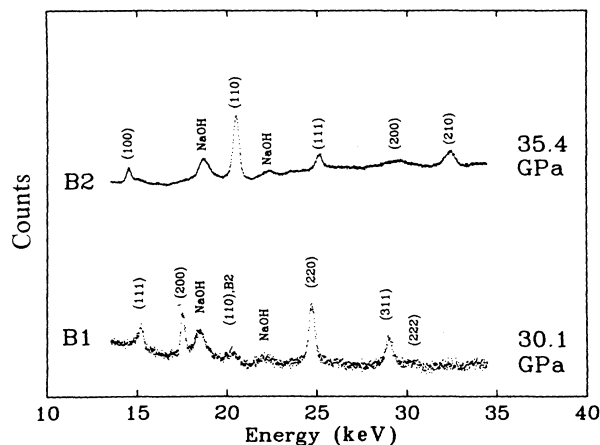


FIG. 1. Energy-dispersive x-ray diffraction patterns of NaH in predominantly $B1$ structure (30.1 GPa) and entirely $B2$ phase (35.4 GPa). The NaOH was formed during sample loading. The peak at 20.5 keV in the $B1$ spectrum is the strongest peak of the $B2$ phase (110), indicating that the transition has begun at this pressure. Both spectra were taken on the CHESS wiggler line with critical energy 25 keV and diffraction angle $\theta = 10.00^\circ$. A background due to Compton scattering from the diamond anvils has been subtracted.

inantly of $B1$ structure and a second at 35.4 GPa with NaH entirely of $B2$ structure. A background due to Compton scattering of the incident beam by the diamond anvils has been subtracted. The presence of NaOH peaks, which remain through the $B1$ -to- $B2$ transition, indicate some formation of NaOH during sample loading. The relative weakness of the (111) and (222) diffraction peaks in the $B1$ structure and the weakness of the (100) and (200) peaks in the $B2$ structure are due to preferred orientation of the NaH crystallites in the sample chamber. At least six diffraction peaks from each structure of NaH were observed at each pressure on the wiggler run. This represents a threefold increase in the number of diffraction peaks observed by us during the hard-bend run, and by Hochheimer *et al.*¹ using a conventional x-ray source. This tripling of the number of diffraction peaks improved the precision with which the lattice constant and equation of state (EOS) were determined, and has provided much greater confidence in the structure assignment.

The $B1$ -to- $B2$ transition started between spectra taken at 28.4 and 30.1 GPa, so we conclude that the uploading transition pressure is 29.3 ± 0.9 GPa at a fractional volume of 0.61 ± 0.01 . The transition was complete on the wiggler run by 35 GPa. With decreasing pressure we observed the reverse $B2$ -to- $B1$ transition at 28.4 ± 2.4 GPa. As discussed below, similar transition pressures have been observed for the Na halides even though NaBr and NaI transform to a distorted $B1$ (GeS-type) structure.⁶ Our data indicates that if a hysteresis exists in NaH between the transition pressures for increasing and decreasing pressure it appears to be smaller than that observed in the other Na salts (transition hysteresis): NaF (6.0 GPa), NaBr (5.5 GPa), and NaI (3.5 GPa).⁶

X-ray irradiation has induced color centers in each NaH preparation, giving the sample a pink-violet color in transmission in the $B1$ phase. At the phase transition this color changes to orange yellow. Pressurizing a third NaH sample to 32 GPa in the absence of x-ray radiation

gave no observable color changes. When this sample was subsequently radiated for 1 h at 24 GPa, the pink-violet color was observed. By 54 GPa the color is fading and optical-absorption data indicates a band gap greater than 3.3 eV.

Figure 2 shows the room-temperature EOS of NaH. The solid curves are Birch first-order⁷ EOS fits to the present data and that of Hochheimer *et al.*¹ The weighting for these nonlinear least-squares fits to pressure-versus-volume fraction is taken as inversely proportional to pressure squared. For the $B1$ phase the bulk modulus $B_0 = 19.4 \pm 2.0$ GPa, and its pressure derivative $B'_0 = 4.4 \pm 0.5$. For the $B2$ phase $B_0 = 28.3 \pm 3.0$ GPa, $B'_0 = 4.3 \pm 0.4$, and its volume extrapolated back to zero pressure divided by its equilibrium $B1$ volume is 0.83 ± 0.04 . The change in volume at 29.3 GPa is 10% of its $B1$ volume at that pressure.

Bashkin *et al.*² have pointed out, using a hard-sphere ion model, that the $B1$ -to- $B2$ transition is thermodynamically possible in NaH, KH, RbH, and CsH. They determined the specific volumes of each phase by summing the metal and hydride ion radii, which depend on the structure and coordination number, to determine the $B2$ lattice constant. They predict² that for LiH the $B1$ structure is more dense than the $B2$ structure at *all* pressures, and will therefore not transform, assuming that the compressibility of the $B1$ phase exceeds that of the $B2$ phase. This assumption is shown to be satisfied for the non-Li alkali hydrides by the present data and by the data of Hochheimer *et al.*¹ The present results eliminate concerns raised for this hard-sphere ion model when the $B1$ -to- $B2$ transition was not observed in NaH to 28 GPa.¹

The $B1$ -to- $B2$ transition pressure for NaH is compared to that for KH, RbH, and CsH in Fig. 3(a), and to the transition pressure from $B1$ for the Na halides in Fig. 3(b). The transition pressure is highly dependent on cation [Fig. 3(a)], but nearly independent of anion [Fig. 3(b)] with all of the Na salts transforming between 26 and 30 GPa.⁶ The strong dependence on cation has also been observed in the alkali-metal halides.⁸ Majewski and Vogal³ have invoked the increasing domination of the total crystal energy by the repulsive overlap energy between the cation s and anion p orbitals as the crystal volume is reduced to qualitatively explain these trends using tight-binding theory. The transition pressure is given by

$$P_T = \frac{\Delta E}{\Delta V}, \quad (1)$$

where ΔE is the change in total crystal energy and ΔV the change in the volume per ion pair. For the $B1$ -to- $B2$ transition in sp -bonded compounds Majewski and Vogal³ find that the denominator of Eq. (1) increases for both increasing cation Z and increasing anion Z . The numerator, however, which is dominated by overlap energies, decreases for increasing cation Z and increases for increasing anion Z . Therefore there is a strong decrease in P_T [Eq. (1)] for increasing cation Z , and a much weaker dependence of P_T on anion Z .

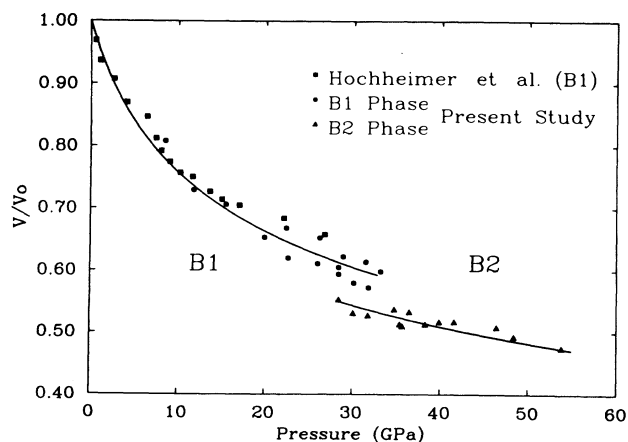


FIG. 2. Room-temperature equation of state of NaH. Solid curves are Birch first-order equation-of-state fits to the combined data of Hochheimer (Ref. 1) and the present data.

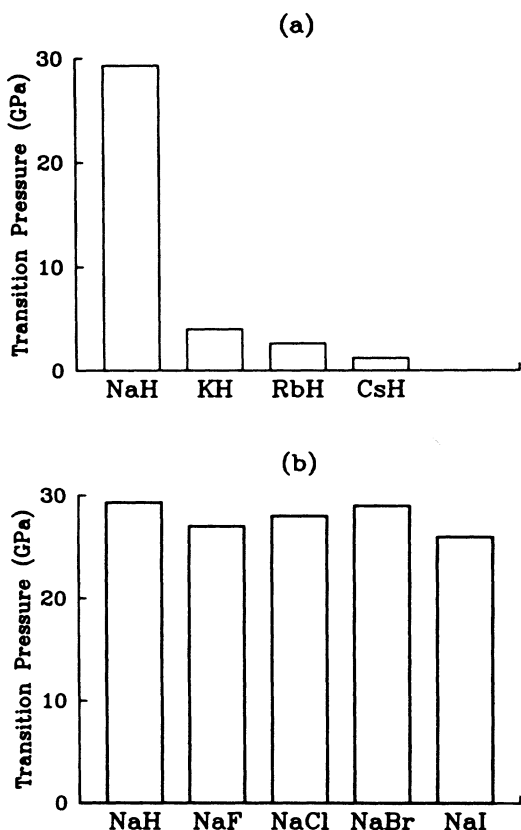


FIG. 3. Comparison of transition-pressure dependence on cation and anion. (a) $B1 \rightarrow B2$ transition for alkali-metal hydrides. (b) $B1 \rightarrow B2$ for NaH, NaF, and NaCl, and $B1 \rightarrow \text{GeS}$ -type for NaBr and NaI.

A more quantitative approach has been taken in the computation of the bulk moduli of the alkali-metal hydrides. Gupta and Kumar⁹ determine the bulk moduli by calculating and differentiating the total crystal energy E :

$$B_0 = V \left. \frac{d^2 E}{dV^2} \right|_{V=V_0} \quad (2)$$

In this theory the energy E is the sum of an electrostatic term

$$E_e = -\frac{\alpha_m e^2}{r}, \quad (3)$$

where α_m is the Madelung constant, an exponential repulsive term calculated from first principles using overlap energies by Hafemeister and Zahart,¹⁰ and a van der Waals term. As Eq. (3) implies, this theory assumes complete charge transfer between the ions in the alkali-metal hydrides.^{9,10} With the present results on NaH, a complete set of experimental bulk moduli of the alkali-metal hydrides is available for the first time for comparison to this theory. This is shown in Table I. The data for LiH are compression measurements made by Stephens and Lilley¹¹ to 4 GPa. The theory is able to

TABLE I. Comparison of experimental and theoretical bulk moduli of the alkali-metal hydrides.

Alkali-metal hydride	Isothermal bulk modulus (GPa)	
	Theory ^a	Experiment
LiH	34.4	34.7 ^b
NaH	22.8	19.4 ± 2.0 ^c
KH	14.8	15.6 ± 1.5 ^d
RbH	12.9	10.0 ± 1.0 ^d
CsH	11.6	7.6 ± 0.8 ^d

^aReference 9.

^bReference 11.

^cPresent work.

^dReference 1.

predict the trends in the bulk moduli as the alkali ion is changed, but the predicted value for CsH, for example, is about 50% too large.

One explanation for this discrepancy may be that the charge transfer in the alkali-metal hydrides is not complete, i.e., the effective charge on each ion is less than $\pm 1e$. There is considerable experimental evidence that supports this conclusion, including trends in the bulk moduli themselves. Figure 4 shows a log-log plot of the bulk modulus versus equilibrium unit-cell volume V_0 for the $B1$ -structured divalent and trivalent rare-earth monochalcogenides, the alkali-metal halides, and the alkali-metal hydrides. Anderson and Nafe¹² and Jayaraman *et al.*,¹³ have shown that the linear behavior observed can be explained with an ionic model incorporating effective ion charges. It is shown that

$$\ln(B_0) = y \ln(V_0) + \ln(Z_1^* Z_2^*) + \text{const}, \quad (4)$$

where the slope y is observed to be -1.1 ± 0.1 for the monochalcogenides and the alkali halides, and the offset is related to the effective charges $Z_1^* Z_2^*$ of the ions.¹³ For the alkali-metal hydrides the slope is -0.97 , and the line lies lower than that for the alkali-metal halides,

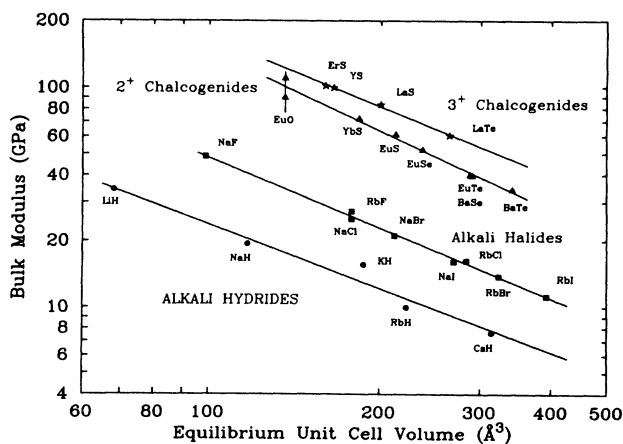


FIG. 4. Bulk moduli at atmospheric pressure of several series of ionic solids in the $B1$ phase. \star , trivalent rare-earth monochalcogenides; \blacktriangle , divalent rare-earth monochalcogenides; and \blacksquare , alkali-metal halides from Ref. 9. \bullet , alkali-metal hydrides: LiH (Ref. 11), NaH (present work), KH, RbH, and CsH (Ref. 1).

indicating the hydrides have an effective charge less than $\pm 1e$ on each ion. Following the notation of Jayaraman¹³ we calculate the effective charge, Z_{eff} , of the alkali-metal hydride ions to be

$$Z_{\text{eff}} = (Z_1^* Z_2^*)^{1/2} = \left(\frac{B}{B_A} \right)^{1/2} = 0.73 \pm 0.03, \quad (5)$$

where B/B_A is the bulk-modulus ratio of the alkali-metal hydrides over the alkali-metal halides, which are assumed to have complete charge transfer. Incomplete charge transfer is consistent with the smaller difference in electronegativities for the alkali hydrides than for the alkali halides. X-ray measurements have shown that LiH is 80–100% ionic,¹⁴ and neutron-diffraction studies indicate 87.5% ionic bonding in LiD.¹⁵ It is also interesting to note that Hartree-Fock calculations indicate an effective charge transfer of $0.78e$ for the LiH molecule.¹⁶ The present results indicate that *all* of the

alkali-metal hydrides, not just LiH, have incomplete charge transfer.

Therefore, a successful theoretical treatment of the alkali-metal halides must take incomplete charge transfer into account. In Born-Mayer model calculations this will affect not only the electrostatic term [i.e., Eq. (3)], but also the repulsive term since the overlap integrals will be modified by the assumption of incomplete charge transfer. We might expect greater success from theories that require no *a priori* assumptions of ionicity, such as the tight-binding theory of Majewski and Vogl.³

We wish to thank the National Science Foundation for its support through Grant No. DMR-86-12289. One of us (S.J.D.) thanks IBM for support. We acknowledge the assistance of Keith E. Brister, Serge Desgreniers, Samuel T. Weir, and the entire CHES staff.

¹H. D. Hochheimer, K. Strossner, W. Honle, B. Baranowski, and F. Filipek, *Z. Phys. Chem.* **143**, 139 (1985).

²I. O. Bashkin, T. N. Dymova, and E. G. Ponyatovskii, *Phys. Status Solidi* **100**, 87 (1980).

³J. A. Majewski and P. Vogl, *Phys. Rev. Lett.* **57**, 1366 (1986).

⁴H. K. Mao, P. M. Bell, J. Shaner, and D. Steinberg, *J. Appl. Phys.* **49**, 3276 (1978).

⁵K. E. Brister, Y. K. Vohra, and A. L. Ruoff, *Rev. Sci. Instrum.* **57**, 2560 (1986).

⁶T. Yagi, T. Suzuki, and S.-I. Akimoto, *J. Phys. Chem. Solids* **44**, 135 (1983).

⁷F. Birch, *J. Geophys. Res.* **83**, 1257 (1978).

⁸C. W. F. T. Pistorius, *Prog. Solid State Chem.* **11**, 1 (1976).

⁹B. R. K. Gupta and V. Kumar, *Czech. J. Phys. B* **33**, 1011 (1983).

¹⁰D. W. Hafemeister and J. D. Zahrt, *J. Chem. Phys.* **47**, 1747 (1965).

¹¹D. R. Stephens and E. M. Lilley, *J. Appl. Phys.* **39**, 177 (1968).

¹²O. L. Anderson and J. E. Nafe, *J. Geophys. Res.* **70**, 3951 (1965).

¹³A. Jayaraman, B. Batlogg, R. G. Maines, and H. Bach, *Phys. Rev. B* **26**, 3347 (1982).

¹⁴R. S. Calder, W. Cochran, D. Griffiths, and R. D. Lowde, *J. Phys. Chem. Solids* **23**, 621 (1962).

¹⁵J. L. Verble, J. L. Warren, and J. L. Yarnell, *Phys. Rev.* **168**, 980 (1968).

¹⁶H. F. King and R. E. Stanton, *J. Chem. Phys.* **50**, 3789 (1969).